RESEARCH ARTICLE

Shuxuetong injection protects cerebral microvascular endothelial cells against oxygen-glucose deprivation reperfusion

Zuo-Yan Sun[1, 2], Fu-Jiang Wang[1], Hong Guo[1], Lu Chen[1], Li-Juan Chai[1], Rui-Lin Li[1], Li-Min Hu[1], Hong Wang[1], Shao-Xia Wang[1, 3, 4, *]
1 Tianjin State Key Laboratory of Modern Chinese Medicine, Tianjin University of Traditional Chinese Medicine, Tianjin, China
2 Department of Pharmacy, Linyi Central Hospital, Linyi, Shandong Province, China
3 School of Integrative Medicine, Tianjin University of Traditional Chinese Medicine, Tianjin, China
4 Key Laboratory of Pharmacology of Traditional Chinese Medical Formula, Ministry of Education, Tianjin University of Traditional Chinese Medicine, Tianjin, China

Funding: *This study was supported in part by the National Natural Science Foundation of China, No. 81573644 (to LMH), 81573733 (to SWX); the Tianjin 131 Innovative Team Project, China (to HW); the National Major Science and Technology Project of China, No. 2012ZX09101201-004 (to SWX); the Science and Technology Plan Project of Tianjin of China, No. 16PTSYJC00120 (to LMH); the Applied Foundation and Frontier Technology Research Program of Tianjin of China (General Project), No. 14JCYBJC28900 (to SXW); the National International Science and Technology Cooperation Project of China, No. 2015DFA30430 (to HW); the Key Program of the Natural Science Foundation of Tianjin of China, No. 16ICZDJC36300 (to HW); the Scientific Research and Technology Development Plan Project of Guangxi Zhuang Autonomous Region of China, No. 14125008-2-5 (to SXW).*

Graphical Abstract

Protective effects of *Shuxuetong* (SXT) injection on cerebral microvascular endothelial cells induced by oxygen-glucose deprivation/reperfusion (OGD/R)

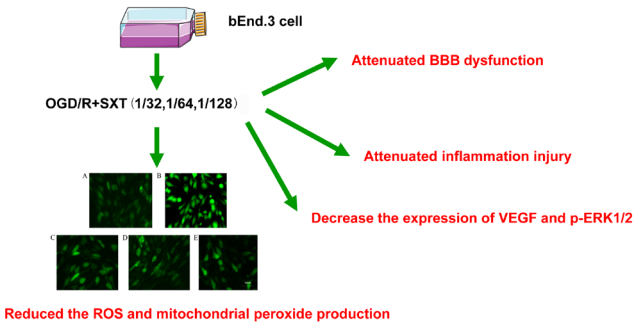

Correspondence to:
Shao-Xia Wang, MD, wangshaoxia1@163.com.

orcid:
0000-0002-1762-8684 (Shao-Xia Wang)

doi: *10.4103/1673-5374.249226*

Received: *March 30, 2018*
Accepted: *July 14, 2018*

Abstract

Shuxuetong injection composed of leech (*Hirudo nipponica Whitman*) and earthworm (*Pheretima aspergillum*) has been used for the clinical treatment of acute stroke for many years in China. However, the precise neuroprotective mechanism of *Shuxuetong* injection remains poorly understood. Here, cerebral microvascular endothelial cells (bEnd.3) were incubated in glucose-free Dulbecco's modified Eagle's medium containing 95% N_2/5% CO_2 for 6 hours, followed by high-glucose medium containing 95% O_2 and 5% CO_2 for 18 hours to establish an oxygen-glucose deprivation/reperfusion model. This *in vitro* cell model was administered *Shuxuetong* injection at 1/32, 1/64, and 1/128 concentrations (diluted 32-, 64-, and 128-times). Cell Counting Kit-8 assay was used to evaluate cell viability. A fluorescence method was used to measure lactate dehydrogenase, and a fluorescence microplate reader used to detect intracellular reactive oxygen species. A fluorescent probe was also used to measure mitochondrial superoxide production. A cell resistance meter was used to measure transepithelial resistance and examine integrity of monolayer cells. The fluorescein isothiocyanate-dextran test was performed to examine blood-brain barrier permeability. Real-time reverse transcription polymerase chain reaction was performed to analyze mRNA expression levels of tumor necrosis factor alpha, interleukin-1β, interleukin-6, and inducible nitric oxide synthase. Western blot assay was performed to analyze expression of caspase-3, intercellular adhesion molecule 1, vascular cell adhesion molecule 1, occludin, vascular endothelial growth factor, cleaved caspase-3, B-cell lymphoma 2, phosphorylated extracellular signal-regulated protein kinase, extracellular signal-regulated protein kinase, nuclear factor-κB p65, I kappa B alpha, phosphorylated I kappa B alpha, I kappa B kinase, phosphorylated I kappa B kinase, claudin-5, and zonula occludens-1. Our results show that *Shuxuetong* injection increases bEnd.3 cell viability and B-cell lymphoma 2 expression, reduces cleaved caspase-3 expression, inhibits production of reactive oxygen species and mitochondrial superoxide, suppresses expression of tumor necrosis factor alpha, interleukin-1β, interleukin-6, inducible nitric oxide synthase mRNA, intercellular adhesion molecule-1, and vascular cell adhesion molecule-1, markedly increases transepithelial resistance, decreases blood-brain barrier permeability, upregulates claudin-5, occludin, and zonula occludens-1 expression, reduces nuclear factor-κB p65 and vascular endothelial growth factor expression, and reduces I kappa B alpha, extracellular signal-regulated protein kinase 1/2, and I kappa B kinase phosphorylation levels. Overall, these findings suggest that *Shuxuetong* injection has protective effects on brain microvascular endothelial cells after oxygen-glucose deprivation/reperfusion. Moreover, its protective effect is associated with reduction of mitochondrial superoxide production, inhibition of the inflammatory response, and inhibition of vascular endothelial growth factor, extracellular signal-regulated protein kinase 1/2, and the nuclear factor-κB p65 signaling pathway.

Key Words: *nerve regeneration; Shuxuetong injection; brain microvascular endothelial cells; oxygen-glucose deprivation/reperfusion; tight junction proteins; mitochondrial function; inflammatory factors; blood-brain barrier; neuroprotection; neural regeneration*

Chinese Library Classification No. *R453; R364; Q26*

Introduction

Ischemic stroke accounts for 75–80% of all strokes and is a leading cause of death and disability. Ischemic stroke is induced by clogged blood vessels that leave target organs at risk of cellular death (Johnston et al., 2009; Roger et al., 2012). Moreover, ischemic cerebral injury is accompanied by severe brain dysfunction. In the early phase, insufficient supply of oxygen, glucose, and energy to damaged regions causes rapid cell injury with a large amount of reactive oxygen species produced in mitochondria (Suchadolskiene et al., 2014). Simultaneously, oxygen-poor reactive oxygen species overload can quickly aggravate mitochondrial damage and mitochondrial oxidative phosphorylation, which induces free lipid accumulation (Adibhatla and Hatcher, 2008). This pathological cascade reaction eventually leads to inflammatory reaction, blood-brain barrier (BBB) breakdown, apoptosis, and cell death within minutes (Xing et al., 2012; Zhang et al., 2017).

To date, tissue plasminogen activator is the only effective treatment for rescuing ischemic brain tissue. However, its application is restricted because of limitations, such as a narrow therapeutic window and risk of cerebral hemorrhage, (Moskowitz et al., 2010). Thus, developing new drugs for acute stroke is urgent. Because of failed clinical trials that centered on neurons, more attention is now being given to non-neuronal cell types (Barreto et al., 2011). Consequently, there is much attention on brain microvascular endothelial cells because of their importance in maintaining integrity of BBB structure and function, which is a promising target for intervention in cerebral ischemic injury (Watanabe et al., 2013). Not surprisingly, brain microvascular endothelial cells are considered to play a central role in BBB function, and are responsible for maintaining BBB integrity through expression of tight junction proteins (Yang and Rosenberg, 2011). Occludin, claudin-5, and zonula occludens-1 (ZO-1) are the major proteins associated with BBB function and structure (Gerriets et al., 2009; Tuttolomondo et al., 2014; Krueger et al., 2015). Nonetheless, primary culture of brain microvascular endothelial cells has drawbacks, namely, a tedious research process, cell contamination, and slow growth. The cell line, bEnd.3, has the basic characteristics of brain microvascular endothelial cells (He et al., 2010; Yang and Rosenberg, 2011), and advantages such as a short growth cycle and rapid cell proliferation. Further, expression of BBB characteristics was also detected with bEnd.3 cells. Accordingly, this cell line can replace primary cells for culture (He et al., 2010; Yang and Rosenberg, 2011). Previous studies have suggested that excessive reactive oxygen species and inflammation are main factors in vascular BBB lesions (Kaur and Ling, 2008; da Fonseca et al., 2014; Kawabori and Yenari, 2015). In addition, several signaling molecules such as extracellular signal regulated protein kinase 1/2 (ERK1/2), vascular endothelial growth factor (VEGF), and nuclear factor kappa-B (NF-κB) are involved in tight junction disruption and BBB breakdown (Beker et al., 2015; Hung et al., 2015; Wang et al., 2015).

Shuxuetong injection is a standardized drug applied clinically. It is recorded by the People's Republic of 2015 Edition of Pharmacopoeia, and used extensively for acute cerebral infarction by activating blood circulation and removing blood stasis, which ultimately activates meridians and collaterals. Shuxuetong injection is used clinically for treating the acute phase of ischemic stroke, and had total sales of over $93 million in 2017 in China. *Shuxuetong* injection is composed of leech (*Hirudo nipponica Whitman*) and earthworm (*Pheretima aspergillum*) (Hu et al., 2009; Yin, 2011a; Liu and Qin, 2016). Until now, the main active components were considered to be peptides, glycopeptides, and oligosaccharides (Yin, 2011b; Liu et al., 2015). In this study, we investigated the protective effects and mechanisms of *Shuxuetong* injection on brain microvascular endothelial cells after exposure to oxygen-glucose deprivation/reperfusion (OGD/R) injury. Specifically, we focused on BBB damage, mitochondrial dysfunction, and inflammatory injury to provide a practical examination for the treatment of ischemic stroke.

Materials and Methods

Cell culture

The mouse brain endothelial cell line, bEnd.3, was purchased from ATCC (Manassas, VA, USA). Cells were cultured in Dulbecco's modified Eagle's medium (Corning Laboratories, Corning, NY, USA), supplemented with 10% fetal bovine serum (Gibco, Grand Island, NY, USA), 100 U/mL penicillin, and 100 U/mL streptomycin (Hyclone Laboratories, Logan, UT, USA) at 37°C in a humidified atmosphere mixture of 5% CO_2 and 95% air. The medium was replaced every 2 days.

OGD/R injury model establishment and *Shuxuetong* injection intervention

To mimic cell impairment during ischemic injury *in vitro*, the previously published OGD/R model was used as described, albeit with some modification (Chen et al., 2014; Wang et al., 2014a, b). Briefly, confluent cells were washed twice with pre-warmed phosphate-buffered saline (PBS). The culture medium was replaced with glucose-free Dulbecco's modified Eagle's medium, transferred to an anaerobic chamber (Stemcell, Vancouver, BC, Canada), and flushed with a gas mixture of 95% N_2/5% CO_2 for 6 hours. After OGD, the medium was exchanged for Dulbecco's modified Eagle's medium with high glucose in a humidified atmosphere with 95% air and 5% CO_2 at 37°C for 18-hour reoxygenation and glucose restoration. Controls were incubated with high-glucose Dulbecco's modified Eagle's medium in a normal atmosphere for 24 hours. OGD/R cells were harvested at 24 hours. *Shuxuetong* injection was diluted with Dulbecco's modified Eagle's medium before use in experiments. The effective concentration of *Shuxuetong* injection was separately diluted 32-, 64-, and 128-times, and added to cells during OGD/R.

Cell viability assay

The Cell Counting Kit-8 assay was used to evaluate cell viability, as previously described (Wu et al., 2013; Pan et al., 2017). Briefly, 1×10^5/mL bEnd.3 cells were seeded into 96-well plates. They had reached 90% confluence at the time of OGD/R. After washing once with PBS, Cell Counting Kit-

8 solution (10%) was added to cultures and incubated for 1 hour in the incubator. Absorbance at 450 nm was measured using a microplate reader (Molecular Devices, Sunnyvale, CA, USA).

Lactate dehydrogenase leakage assay

Lactate dehydrogenase released from impaired cells was assessed using a diagnostic kit. bEnd.3 cells were plated into 96-well plates at 1×10^5/mL, and harvested at 80–90% confluence. A small amount of culture medium (50 μL) was transferred into a new plate, and 50 μL of CytoTox-ONE Reagent (Dojindo, Shanghai, China) added and incubated for 10 minutes. Stop solution was then added. Fluorescence with an excitation wavelength of 490 nm was recorded (Molecular Devices).

Intracellular reactive oxygen species levels and superoxide production assays

Intracellular levels of reactive oxygen species production were measured as described previously (Wei et al., 2000). Detection of mitochondrial superoxide was measured using the fluorogenic probe, MitoSOX™ Red (Invitrogen, Carlsbad, CA, USA) (Won et al., 2015). bEnd.3 cells were subjected to OGD for 4 hours, then switched to a reperfusion condition and incubated for 60 minutes. Cells were loaded with 5 μM CM-H2DCFDA (Invitrogen) at 37°C for 10 minutes (reactive oxygen species levels), or 5 μM MitoSOXTM Red (Invitrogen) at 37°C for 30 minutes (superoxide production). Thereafter, cells were washed three times with PBS to remove residual probe. Cellular fluorescence intensity was measured at ex/em wavelengths of 488/525 nm and 510/580 nm, respectively, using a fluorescence microplate reader (Molecular Devices). Expression of fluorescence intensity was expressed as percentage of the control group. Images were captured using an inverted fluorescence microscope (TE200; Nikon, Tokyo, Japan).

Transepithelial electrical resistance assay

Integrity of monolayer bEnd.3 cells was measured using the transepithelial electrical resistance assay (Cao et al., 2016), according to the manufacturer's instructions (Millipore, Billerica, MA, USA). Cells were seeded at 5×10^4/mL in 200 μL complete Dulbecco's modified Eagle's medium in 24-well plates. Transepithelial electrical resistance value was detected using the Millicell ERS-Volt-Ohm Meter (Millipore).

BBB permeability assay

Function of *Shuxuetong* injection in regulating BBB permeability was tested *in vitro* using fluorescein isothiocyanate (FITC)-dextran and cell culture chamber Transwell inserts, as previously described (Shin et al., 2016). FITC-dextran (final concentration 1 mg/mL; average molecular mass 70 kDa; Sigma-Aldrich, St. Louis, MO, USA) was added to the upper culture medium at 37°C for 2 hours, followed by OGD/R. Next, 100 μL medium was collected from the lower compartment and fluorescence intensity measured using a microplate reader at 492/518 nm absorption/emission wavelengths.

Real-time reverse transcription polymerase chain reaction (RT-PCR) assay

After OGD for 6 hours and reperfusion for 18 hours, bEnd.3 cells were harvested from 6-well plates at 2×10^5/mL. Total RNA was extracted using Trizol Reagent (Invitrogen). RNA samples (1 μg) were subsequently reverse-transcribed to cDNA using High Capacity cDNA Reverse Transcription Kits. Briefly, reactions were incubated in steps of 25°C for 10 minutes, 37°C for 120 minutes, 85°C for 5 minutes, and then held at 4°C. RT-PCR was performed using the ABI PRISM 7500 Sequence Detection System (Applied Biosystems, Foster City, CA, USA), with SYBR® Select Master Mix reagent and specific primers (**Table 1**). For each PCR, 20 μL total volumes consisted of 0.8 μL each of specific primer, 2 μg of cDNA template, and 10 μL of 2 × RT master mix. Thermal cycling conditions were: 95°C for 10 minutes, 40 cycles of 95°C for 15 seconds, and extension at 60°C for 1 minute. Fluorescence signal was detected at the end of each cycle. mRNA expression levels were determined relative to a blank control after normalizing to glyceraldehyde 3-phosphate dehydrogenase (GAPDH) using the $2^{-\Delta\Delta CT}$ method. Analysis was performed in triplicates.

Table 1 Primers used for real-time reverse transcription polymerase chain reaction

Genes	Primer/probe	Primer/probe sequences
TNF-α	Forward primer	5′-CGG GGT GAT CGG TCC CCA AAG-3′
	Reverse primer	5′-GGA GGG CGT TGG CGC GCT GG-3′
IL-1β	Forward primer	5′-GAC CTT CCA GGA TGA GGA CA-3′
	Reverse primer	5′-AGC TCA TAT GGG TCC GAC AG-3′
IL-6	Forward primer	5′-CAG AGA TAC AAA GAA ATG ATG G-3′
	Reverse primer	5′-ACT CCA GAA GAC CAG AGG AAA-3′
iNOS	Forward primer	5′-CAC CTT GGA GTT CAC CCA GT-3′
	Reverse primer	5′-ACC ACT CGT ACT TGG GAT GC-3′
GAPDH	Forward primer	5′-CTT CAC CAC CAT GGA GAA GGC-3′
	Reverse primer	5′-GGC ATG GAC TGT GGT CAT GAG-3′

GAPDH: Glyceraldehyde-3-phosphate dehydrogenase; TNF: tumor necrosis factor; IL: interleukin; iNOS: inducible nitric oxide synthase.

Western blot assay

bEnd.3 cells were lysed in the presence of a protease inhibitor (Beyotime, Shanghai, China), and subsequently centrifuged at 12,000 r/min for 30 minutes at 4°C. Proteins were separated by sodium dodecyl sulfate-polyacrylamide gel electrophoresis, and then transferred onto polyvinylidene fluoride membranes (Millipore, Bedford, MA, USA). Membranes were blocked with 5% non-fat milk, followed by 4°C incubation overnight with anti-caspase-3 (rabbit, polyclonal antibody, 1:1000; Abcam, Cambridge, MA, USA), anti-vascular cell adhesion molecule-1 (rabbit, polyclonal antibody, 1:1000; Abcam), anti-intercellular adhesion molecule-1 (mouse, monoclonal antibody, 1:1000; Abcam), anti-occludin (rabbit, monoclonal antibody, 1:1000; Abcam), anti-VEGF antibody (rabbit, monoclonal antibody, 1:1000; Abcam), anti-cleaved caspase-3 (rabbit, monoclonal antibody, 1:800; CST, Beverly, MA, USA), anti-B-cell lymphoma 2 (Bcl-2) (rabbit, monoclonal antibody, 1:1000; CST),

anti-phosphorylated-(p)-ERK (rabbit, monoclonal antibody, 1:1000; CST), anti-ERK (rabbit, monoclonal antibody, 1:1000; CST), anti-NF-κB p65 (rabbit, monoclonal antibody, 1:1000; CST), anti-I kappa B alpha (IκBα) (rabbit, monoclonal antibody, 1:1000; CST), anti-p-IκBα (rabbit, monoclonal antibody, 1:1000; CST), anti-I kappa B kinase (IKK) (rabbit, monoclonal antibody, 1:1000; CST), anti-p-IKK antibody (rabbit, monoclonal antibody, 1:1000; CST), anti-claudin-5 antibody (mouse, monoclonal antibody, 1:1000; Invitrogen), and anti-ZO-1 antibody (rabbit, polyclonal antibody, 1:1000; Millipore). β-Actin (rabbit, monoclonal antibody, 1:4000; CST) and anti-lamin-B1 antibody (rabbit, monoclonal antibody, 1:1000; Abcam) served as internal references. Membranes were incubated with the corresponding secondary antibodies: FITC-conjugated anti-mouse IgG (1:10,000; Zhongshan Company, Beijing, China) or FITC-conjugated anti-rabbit IgG (1:10,000; Zhongshan Company) for 1 hour at room temperature. Signal was visualized by enhanced chemiluminescence (Millipore). Quantification of bands was performed from optical density values using the Quantity One analysis system (Bio-Rad, Hercules, CA, USA).

Statistical analysis

Data are expressed as mean ± SD. All data obtained from at least three repeated experiments were analyzed using IBM SPSS Version 21.0 (IBM SPSS Inc., Chicago, IL, USA). Comparisons between multiple groups were performed by one-way analysis of variance followed by the least significant difference test. A value of $P < 0.05$ was considered statistically significant.

Results

Shuxuetong injection attenuates cell death and affects apoptosis-related protein expression of bEnd.3 cells after OGD/R-induced injury

First, bEnd.3 cells were exposed to 6 hours of OGD followed by 18 hours of reperfusion. Cell viability was assessed by both Cell Counting Kit-8 assay and measurement of extracellular lactate dehydrogenase leakage. As shown in **Figure 1A**, cell viability after 6 hours of OGD/R was reduced compared with the control group ($P < 0.01$). Administration of *Shuxuetong* injection significantly attenuated OGD/R-induced cell death, with significantly increased cell viability at 1/32, 1/64, and 1/128 concentrations compared with the 6-hour OGD/R group (all $P < 0.01$). As shown in **Figure 1B**, leakage of lactate dehydrogenase increased in the OGD/R group compared with the control group ($P < 0.01$). Meanwhile, *Shuxuetong* injection (1/32, 1/64, and 1/128) significantly reduced lactate dehydrogenase leakage (all $P < 0.01$). As shown in **Figure 1C** & **D**, OGD/R markedly increased expression of cleaved caspase-3 protein ($P = 0.018$), while it

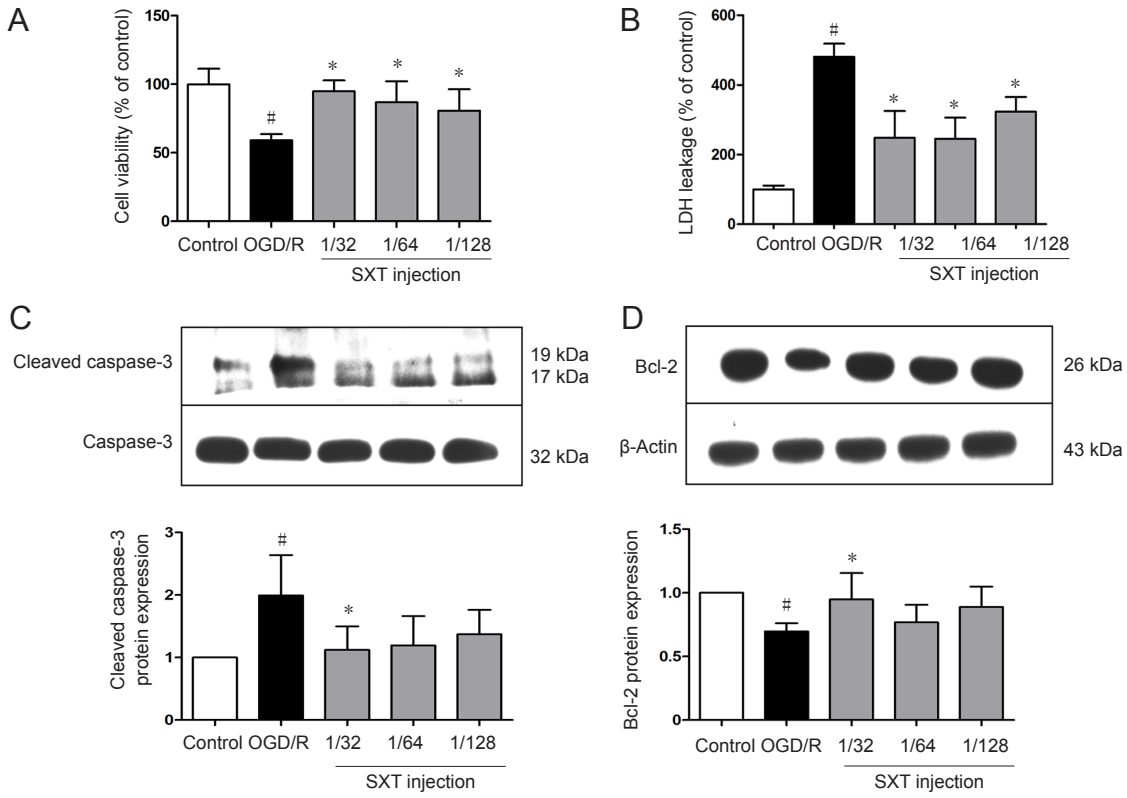

Figure 1 Effect of SXT on cell viability and apoptosis-related protein expression in bEnd.3 cells subjected to OGD/R.
bEnd.3 cells subjected to 6-hour OGD followed by reperfusion for 18 hours were administered *Shuxuetong* injection at 1/32, 1/64, and 1/128 concentrations (diluted 32-, 64-, and 128-times). (A) Cell viability detected by Cell Counting Kit-8 assay was analyzed at 24 hours after OGD/R. (B) LDH leakage detected by fluorescence analysis was analyzed at 24 hours after OGD/R. (C, D) Cleaved caspase-3 and Bcl-2 protein expression detected by western blot assay was analyzed at 24 hours after OGD/R. Relative protein expression was expressed as optical density value relative to control group after normalizing to GAPDH optical density value. Data are expressed as the mean ± SD (mean from three independent experiments, one-way analysis of variance followed by the least significant difference test). #$P < 0.05$, *vs.* control group; *$P < 0.05$, *vs.* OGD/R group ($n = 6$). SXT: *Shuxuetong* injection; OGD/R: oxygen-glucose deprivation/reperfusion; LDH: lactate dehydrogenase GAPDH: glyceraldehyde-3-phosphate dehydrogenase.

was significantly attenuated by *Shuxuetong* injection treatment ($P < 0.05$ with 1/32 and 1/64 concentrations) (**Figure 1C**). Bcl-2 protein expression was reduced in the OGD/R group compared with the control group ($P = 0.021$), and significantly increased with *Shuxuetong* injection treatment ($P < 0.05$ with 1/32 concentration) (**Figure 1D**).

Further, we observed morphological changes after OGD/R injury. Consequently, after OGD for 6 hours and reperfusion for 18 hours, some bEnd.3 cells displayed shrinking bodies, and overall cells were sparse in the OGD/R group compared with the control group. However, *Shuxuetong* injection treatment at different concentrations (1/32, 1/64, and 1/128) attenuated OGD/R-induced injury to cellular morphology. Specifically, cells exhibited relatively good adherence compared with the OGD/R group (**Figure 2**).

Shuxuetong injection reduces reactive oxygen species and mitochondrial superoxide production of bEnd.3 cells after OGD/R-induced injury

Reactive oxygen species and mitochondrial superoxide levels were measured using DCFH-DA and MitoSOXTM Red reagents to determine whether *Shuxuetong* injection can exert a protective effect by inhibiting oxidative stress. bEnd.3 cells were exposed to 4 hours of OGD followed by reperfusion for 1 hour. As shown in **Figure 3A** & **B**, production of reactive oxygen species and mitochondrial superoxide in cells was increased (both $P < 0.01$) compared with controls. Administration of *Shuxuetong* injection significantly attenuated reactive oxygen species levels and mitochondrial superoxide production compared with the OGD/R group (all $P < 0.05$) (**Figure 3C** & **D**).

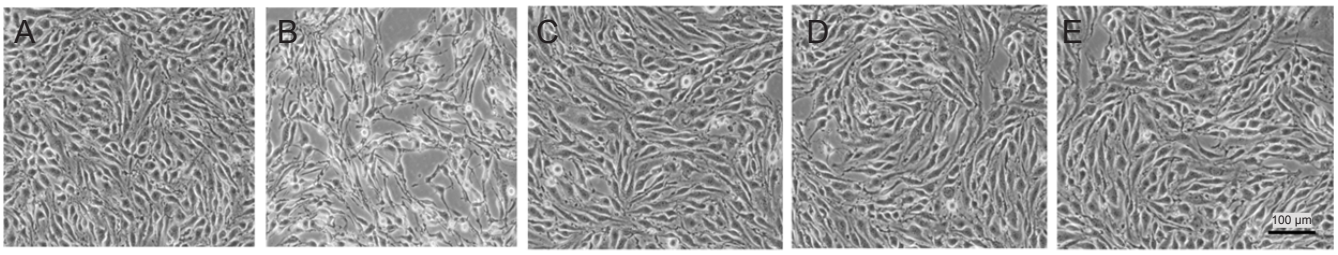

Figure 2 Change in morphology of bEnd.3 cells treated with different concentrations of SXT followed by OGD/R.
(A) Control group; (B) OGD/R group; (C–E) SXT at concentrations of 1/32, 1/64, and 1/128 (diluted 32-, 64-, and 128-times) with OGD injury for 6 hours and reperfusion for 18 hours. bEnd.3 cells displayed normal cell morphology in the control group (A), while cells were sparse with shrinking bodies in the model group (B). Treatment with SXT at different concentrations (1/32, 1/64, and 1/128) (C–E) resulted in relatively good adherence compared with cells in the model group. Scale bar: 100 μm. SXT: *Shuxuetong* injection; OGD/R: oxygen-glucose deprivation/reperfusion.

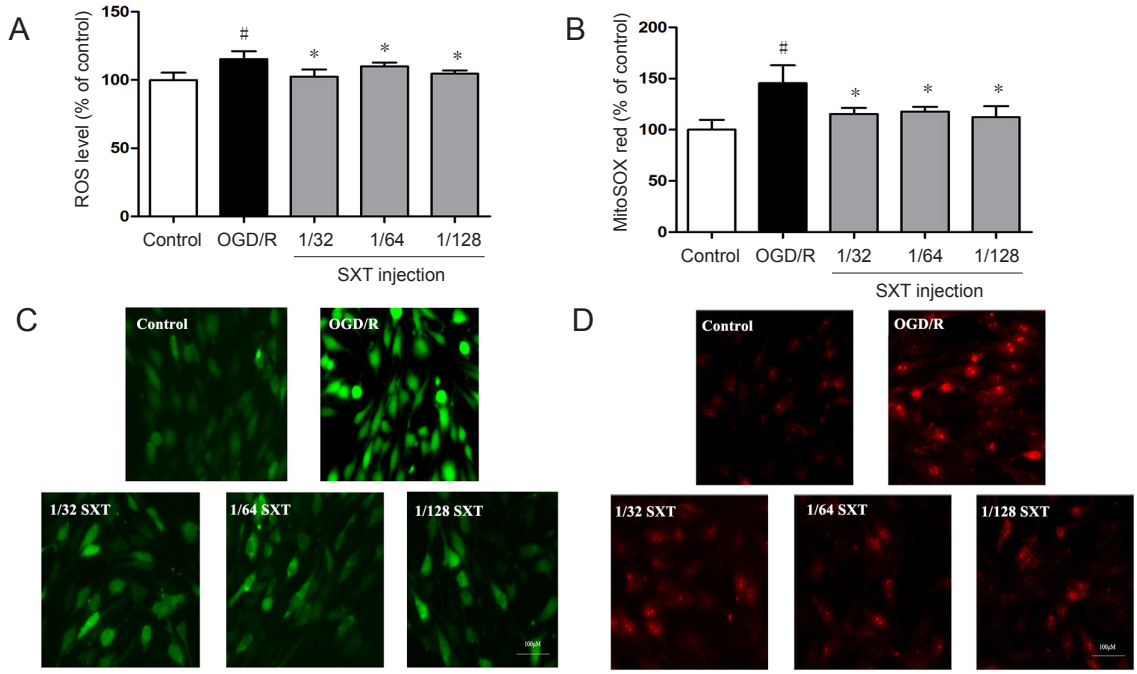

Figure 3 Effect of SXT on ROS and mitochondrial peroxide production in bEnd.3 cells subjected to OGD/R.
(A, B) Intracellular ROS levels (A) and mitochondrial superoxide levels (B) detected by fluorescence analysis. Intracellular ROS levels or mitochondrial superoxide levels were expressed as fluorescence intensity percentage of control group. Data are expressed as the mean ± SD (mean from three independent experiments; one-way analysis of variance followed by the least significant difference test). #$P < 0.05$, *vs.* control group; *$P < 0.05$ *vs.* OGD/R group ($n = 6$). (C, D) Representative images of ROS (green) (C) and MitoSOX™ Red (red) (D). Scale bars: 100 μm. SXT: *Shuxuetong* injection; OGD/R: oxygen-glucose deprivation/reperfusion; ROS: reactive oxygen species.

***Shuxuetong* injection attenuates inflammation injury in bEnd.3 cells after OGD/R-induced injury**

OGD/R injury can trigger inflammation and induce various inflammatory mediators (Moskowitz et al., 2010). Next, we examined gene expression of proinflammatory cytokines such as TNF-α, interleukin (IL)-6, IL-1β, and inducible nitric oxide synthase by RT-PCR, and detected expression of intercellular adhesion molecule-1 and vascular cell adhesion molecule-1 by western blot assay. Our other results (*i.e.*, reactive oxygen species levels, mitochondrial superoxide levels, and transepithelial electrical resistance) clearly show a dose-response relationship with *Shuxuetong* injection. Thus, an optimal concentration (1/32) was chosen to examine mRNA levels. Although only one concentration was used, our data still suggests that *Shuxuetong* injection inhibits expression of inflammatory factors in bEnd.3 cells subjected to OGD/R injury. Accordingly, our results showed that *Shuxuetong* injection suppresses expression of intercellular adhesion molecule-1 ($P < 0.05$ at 1/64 concentration) and vascular cell adhesion molecule-1 ($P < 0.05$ with all three concentrations). Furthermore, expression of TNF-α, IL-6, IL-1β, and mRNA was remarkably increased after OGD/R-induced injury compared with controls (all $P < 0.05$). This increasing trend of inflammatory factors was inhibited by *Shuxuetong* injection at a concentration of 1/32 (all $P < 0.05$). Altogether, these data suggest that *Shuxuetong* injection inhibits expression of inflammatory factors in bEnd.3 cells subjected to OGD/R injury (**Figure 4**).

***Shuxuetong* injection attenuates BBB dysfunction in bEnd.3 cells after OGD/R-induced injury**

To examine BBB integrity and permeability of monolayer bEnd.3 cells, the transepithelial electrical resistance assay and FITC-dextran assay were used, respectively. As shown in **Figure 5**, transepithelial electrical resistance was decreased to 59.26 ± 4.66% after OGD/R-induced injury compared with the control group ($P < 0.01$). Administration with *Shuxuetong* injection significantly increased transepithelial electrical resistance to 120.43 ± 5.22%, 114.30 ± 3.74%, and 113.67 ± 4.29% at concentrations of 1/32, 1/64, and 1/128, respectively, compared with the OGD/R group (all $P < 0.01$). As shown in **Figure 3B**, FITC-dextran concentration detected by cell culture chamber Transwell inserts increased to 143.69 ± 8.36% after OGD/R-induced injury compared with the control group ($P < 0.01$). Correspondingly, *Shuxuetong* injection reduced FITC-dextran concentration ($P < 0.05$ with 1/32 and 1/64 concentrations). These results suggest that *Shuxuetong* injection can protect bEnd.3 cells from damage by protecting the BBB.

***Shuxuetong* injection improves expression of tight junction proteins in bEnd.3 cells after OGD/R-induced injury**

Aside from detecting BBB integrity and permeability, we also investigated the effect of *Shuxuetong* injection on expression of tight junction proteins after OGD/R injury. Compared with the control group, OGD/R visibly decreased expression of claudin-5, occludin, and ZO-1 in bEnd.3 cells (all $P < 0.05$). Administration of *Shuxuetong* injection significantly increased expression of claudin-5 (all $P < 0.05$), occludin (all $P < 0.05$), and ZO-1 ($P < 0.05$ with concentrations of 1/32 and 1/64) (**Figure 6**). These results show that *Shuxuetong* injection protects tight junction protein degradation following OGD/R injury.

***Shuxuetong* injection inhibits activation of NF-κB in bEnd.3 cells after OGD/R injury**

To further investigate whether NF-κB transcription factors are involved in the protective effect of *Shuxuetong* injection against OGD/R injury, we measured translocation of NF-κB p65 and p-IκBα and p-IKK changes in bEnd.3 cells after OGD, with or without *Shuxuetong* injection treatment. Western blot assay results showed significantly increased protein levels of nuclear NF-κB p65, and IκBα and IKK phosphorylation levels, in bEnd.3 cells after OGD/R treatment compared with the control group (all $P < 0.05$). This tendency was substantially reduced in bEnd.3 cells by administration of *Shuxuetong* injection at concentrations of 1/32, 1/64, and 1/128. Significance was detected for protein levels of nuclear NF-κB p65 ($P < 0.05$ at 1/64 concentration) and phosphorylation levels of IκBα ($P < 0.05$ at 1/32 concentration) and IKK ($P < 0.05$ at 1/64 and 1/128 concentrations). Total protein levels of NF-κB p65 showed no obvious change in bEnd.3 cells induced by OGD/R ($P > 0.05$) (**Figure 7**). NF-κB p65 translocates from the cytoplasm to nucleus. Thus, these results suggest that *Shuxuetong* injection inhibits activation of the NF-κB pathway.

***Shuxuetong* injection decreases VEGF and p-ERK1/2 expression after OGD/R-induced injury**

OGD/R induces destruction or rearrangement of tight junctions, which further leads to an increase in BBB permeability. Factors involved include levels of signaling molecules such as pERK1/2 and the downstream molecule VEGF. bEnd.3 cells were exposed to 6-hour OGD and 18-hour reperfusion. Expression of VEGF protein and p-ERK1/2 were determined. As shown in **Figure 8**, expression of VEGF ($P = 0.04$) and phosphorylation of ERK1/2 ($P = 0.041$) were increased in the OGD/R group compared with the control group, and this increase was reversed by *Shuxuetong* injection. These results show that OGD/R-induced BBB disruption and the subsequent effect of *Shuxuetong* injection are associated with regulating signaling molecules of VEGF (all $P < 0.05$) and p-ERK1/2 ($P < 0.05$ with 1/32 and 1/128 concentrations).

Discussion

Shuxuetong injection is a traditional Chinese animal medicine that contains leech (*Hirudo nipponica Whitman*) and earthworm (*Pheretima aspergillum*), and is approved by the Chinese National Drug Administration. The manufacturing technology involves impregnating leeches and earthworms, which are then chopped and homogenized into slices, and repeatedly frozen. Afterwards, the slices are centrifuged and ultrafiltrated using freeze-thaw fluid to obtain a rough fil-

tration. Subsequent injection is complicated by mixing two types of extracts. In recent years, pharmacological studies have shown that *Shuxuetong* injection exerts a significant effect on reducing total cholesterol, anticoagulation and fibrinolysis, reducing blood viscosity, and improving hemodynamics for combating ischemic stroke in clinical cases (Hu et al., 2009; Yin, 2011a; Liu and Qin, 2016). However, the specific effects of *Shuxuetong* injection on ischemic pathological injury have not yet been defined in basic experimental studies. Moreover, the specific mechanism of *Shuxuetong* injection's effect is far from clear and needs further investigation. In this study, we used the classical OGD/R-induced endothelial cell injury model to identify protective effects and possible mechanisms of *Shuxuetong* injection after ischemic stroke *in vitro*.

Previous studies have shown that structural and functional integrity of the BBB is compromised by dysfunction of microvascular endothelial cells after OGD/R injury (Sandoval and Witt, 2008; Engelhardt and Liebner, 2014). Accordingly, our study shows that administration of *Shuxuetong* injection prevents reduction of transepithelial electrical resistance and increases permeation of FITC-dextran, suggesting that *Shuxuetong* injection plays a possible protective function in modulating BBB permeability following OGD/R insult. Additionally, BBB integrity depends on degradation and/or redistribution in brain endothelial cells of tight junction proteins such as claudin-5, occludin, and ZO-1 (Kago et al., 2006; Zehendner et al., 2011; Xu et al., 2012). Here, we found an obvious decrease in claudin 5, occludin, and ZO-1 expression in bEnd.3 cells after OGD/R insult. Meanwhile, *Shuxuetong* injection prevented transepithelial electrical resistance reduction and increased permeation of FITC–dextran, thereby upregulating expression of tight junction proteins after OGD/R. Altogether, this shows that *Shuxuetong* injection plays a neuroprotective role in protecting the BBB and maintaining environmental stability in the central nervous system after acute cerebral ischemia. Our experimental results suggest that *Shuxuetong* injection prohibits cellular necrosis and apoptosis though the redox signaling pathway.

Oxidative stress reactions (including reactive oxygen species, mitochondrial superoxide, and inflammatory factors) are generated during ischemic stroke, and are a significant contributor to disruption of the BBB and eventual increase in brain damage (Pan and Kastin, 2007; Li et al., 2009; Amantea et al., 2015). These findings led us to determine if there is a protective effect of *Shuxuetong* injection on OGD/R-induced reactive oxygen species, mitochondrial superoxide production, and inflammatory cytokine secretion. Our results show that production of reactive oxygen species, mitochondrial superoxide, and inflammatory cytokine expression are increased in brain endothelial cells after OGD/R exposure. Further, the effects of these increases decreased after *Shuxuetong* injection treatment.

Several assumptions have been proposed to explain the underlying mechanisms of BBB dysfunction *via* expression of tight junction proteins after OGD/R injury. For example, upregulation of VEGF and ERK1/2 and activation of the NF-κB signaling pathway have been suggested (**Figure 9**) (Coisne et al., 2007; Kuhlmann et al., 2009; Blum et al., 2012; Engelhardt et al., 2014). ERK1/2 phosphorylation participates in degradation of tight junction protein levels in cerebral microvascular endothelial cells after ischemic stimuli (Shin et al., 2015b). Activation of VEGF is associated with tight junction protein levels in brain endothelial cells under chemical hypoxia *in vitro* (Shin et al., 2015a). Upregulation of VEGF expression can be induced by cerebral ischemia reperfusion injury, which is a key regulator for increasing BBB permeability (Young et al., 2004), while inhibition of VEGF expression can reduce BBB damage (Zhang et al., 2000). Protein levels of VEGF were increased followed by increasing pERK1/2 expression, and could be inhibited by the ERK1/2 inhibitor, U0126, after ischemic injury in neonatal rat brain, suggesting that ERK1/2 participates in regulation of VEGF levels (Li et al., 2008). In contrast, changes of VEGF in brain endothelial cells after OGD/R exposure were dependent on ERK1/2 activation (Narasimhan et al., 2009). These results suggest that the preventative effect of *Shuxuetong* injection on degradation of tight junction proteins is associated with mechanisms underlying VEGF and p-ERK1/2 expression.

In addition, another study noted that NF-κB is also a key protein in endothelial barrier disruption (Preston et al., 2002). Our results show that *Shuxuetong* injection inhibits NF-κB activation, suggesting that *Shuxuetong* injection protects BBB dysfunction by inhibiting activation of the molecular mechanism for NF-κB.

In summary, *Shuxuetong* injection reduces reactive oxygen species and mitochondrial superoxide production, inhibits inflammatory cytokine expression, and protects against BBB leakage by protecting tight junction protein expression levels. A possible mechanism may be that *Shuxuetong* injection can regulate NF-κB, VEGF, and ERK1/2 levels, and consequently exert a protective effect on BBB dysfunction in cerebral microvascular endothelial cells exposed to OGD/R injury. However, our study has limitations. For example, the dose-effect relationship of *Shuxuetong* injection injection is not very distinct, while the effective component(s) of *Shuxuetong* injection injection are still not clear. In follow-up experiments, it is necessary to investigate the effect of *Shuxuetong* injection on the protective effect of cerebral ischemia, as well as the corresponding dose-effect relationship. Pharmacology organically combines with drug chemistry, drug analysis, and other disciplines. This study clarifies the effective material basis of *Shuxuetong* injection to provide an experimental basis for its clinical application.

Author contributions: *All authors contributed to conception and design of this study, performed the experiments, participated in data collection and analysis, contributed to preparation of manuscript, and approved the final version of the paper.*
Conflicts of interest: *The authors declare having no conflicts of interest pertinent to the current study and manuscript.*
Financial support: *This study was supported in part by the Nation-*

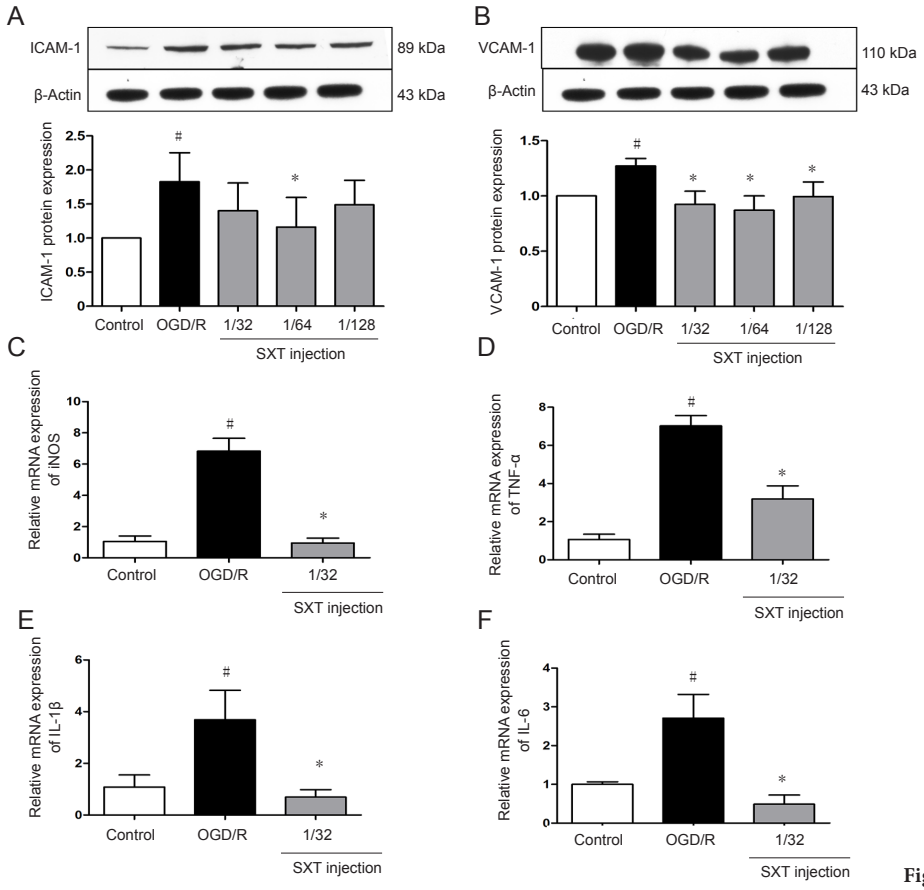

Figure 4 Effect of SXT on expression of inflammatory cytokines induced in bEnd.3 cells by OGD/R injury.
Cells subjected to 6-hour OGD followed by reperfusion for 18 hours were administered *Shuxuetong* injection at 1/32, 1/ 64, and 1/128 concentrations (diluted 32-, 64-, and 128-times). (A, B) ICAM-1 and VCAM-1 protein expression levels were detected by western blot assay. Relative protein expression was expressed as optical density value relative to the control group after normalizing to β-actin optical density value. (C–F) iNOS, TNF-α, IL-1β, and IL-6 mRNA expression levels were detected by real-time polymerase chain reaction. mRNA expression levels were determined relative to a blank control after normalizing to GAPDH using the $2^{-\Delta\Delta CT}$ method. Data are expressed as the mean ± SD (mean from three independent experiments; one-way analysis of variance followed by the least significant difference test). #*P* < 0.05, *vs*. control group; ∗*P* < 0.05, *vs*. OGD/R group (*n* = 3). SXT: *Shuxuetong* injection; OGD/R: oxygen-glucose deprivation/reperfusion; ICAM-1: intercellular adhesion molecule-1; VCAM-1: vascular cell adhesion molecule-1; TNF: tumor necrosis factor; IL: interleukin; iNOS: inducible nitric oxide synthase; GAPDH: glyceraldehyde-3-phosphate dehydrogenase.

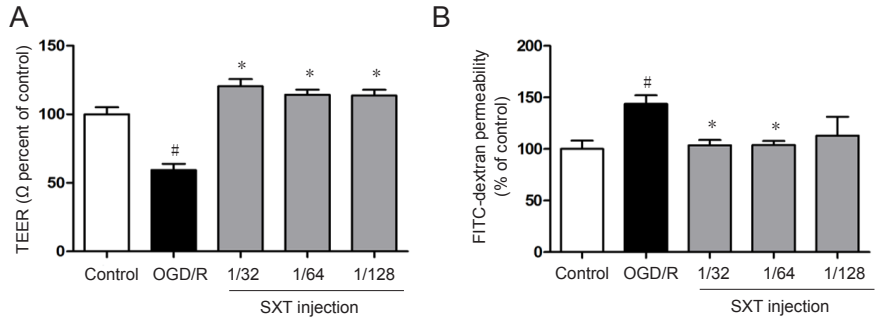

Figure 5 Effect of SXT on blood-brain barrier function in bEnd.3 cells after OGD/R injury.
Cells subjected to 6-hour OGD followed by reperfusion for 18 hours were administered *Shuxuetong* injection at 1/32, 1/ 64, and 1/128 concentrations (diluted 32-, 64-, and 128-times). (A) TEER values in monolayer bEnd.3 cells were detected using a cell resistance meter. (B) Quantification of FITC-dextran values detected by a microplate reader to measure blood-brain barrier permeability. Data are expressed as the mean ± SD (mean from three independent experiments; one-way analysis of variance followed by the least significant difference test). #*P* < 0.05, *vs*. control group; ∗*P* < 0.05, *vs*. OGD/R group (*n* = 6). SXT: *Shuxuetong* injection; OGD/R: oxygen-glucose deprivation/reperfusion; TEER: transepithelial electrical resistance; FITC: fluorescein isothiocyanate.

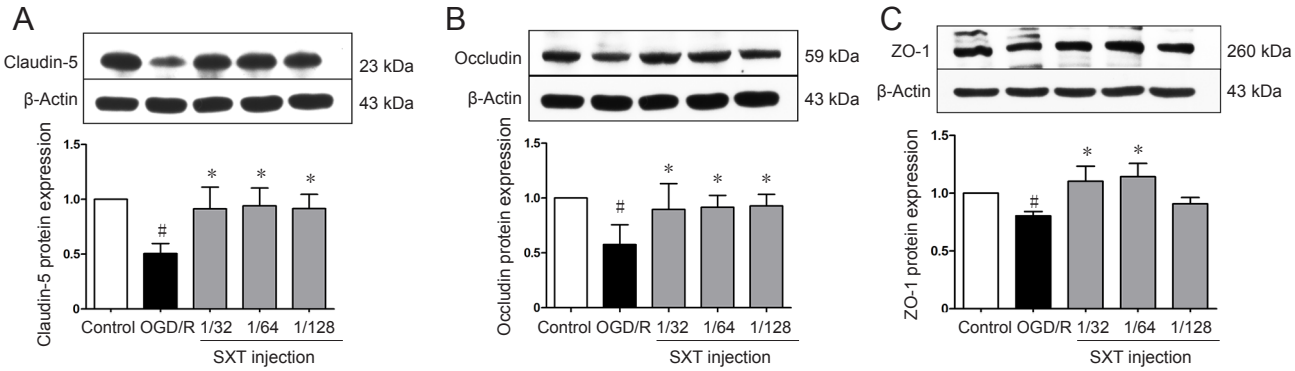

Figure 6 Effect of SXT on protein expression of tight junction proteins in bEnd.3 cells after OGD/R injury.
Cells subjected to 6-hour OGD followed by reperfusion for 18 hours were administered *Shuxuetong* injection at 1/32, 1/ 64, and 1/128 concentrations (diluted 32-, 64-, and 128-times). Protein expression levels of (A) claudin-5, (B) occludin, and (C) ZO-1 levels were measured by western blot assay. Relative protein expression was expressed as optical density value relative to control group after normalizing to β-actin optical density value. Data are expressed as the mean ± SD (mean from three independent experiments; one-way analysis of variance followed by the least significant difference test). #*P* < 0.05, *vs*. control group; ∗*P* < 0.05, *vs*. OGD/R group (*n* = 6). SXT: *Shuxuetong* injection; OGD/R: oxygen-glucose deprivation/reperfusion; zo-1: zonula occludens-1.

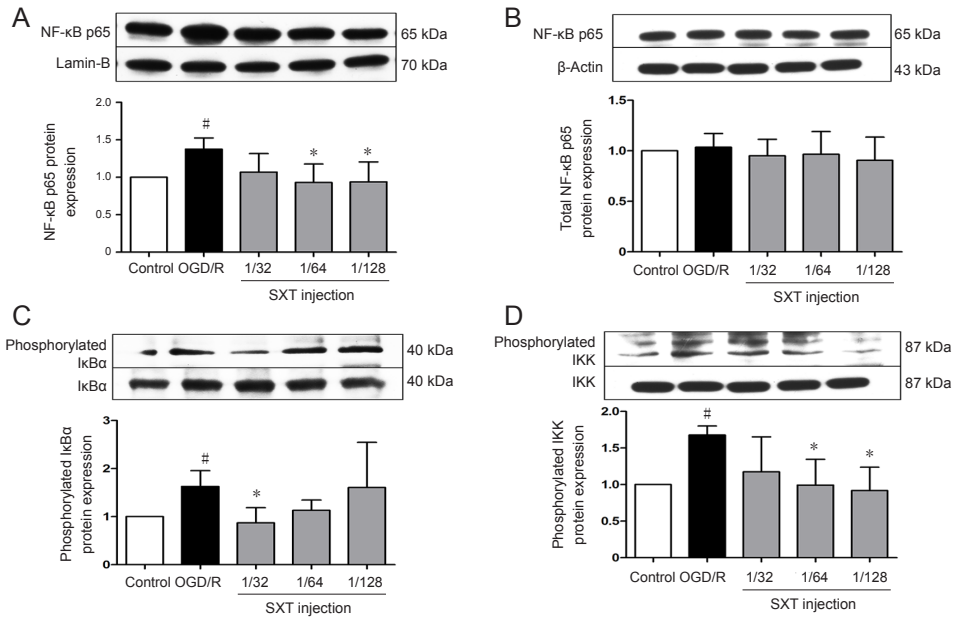

Figure 7 Effect of SXT on NF-κB signal activation in bEnd.3 cells after OGD/R.

Cells subjected to 6-hour OGD followed by reperfusion for 18 hours were administered *Shuxuetong* injection at 1/32, 1/ 64, and 1/128 concentrations (diluted 32-, 64-, and 128-times). Protein levels of nuclear NF-κB p65 (A), cytoplasmic NF-κB p65 (B), phosphorylated IκBα (C), and phosphorylated IKK (D) were detected by western blot assay. NF-κB p65 protein in the cytoplasm and nucleus were expressed as a relative ratio of target protein to β-actin or lamin-B respectively. Protein levels of phosphorylated IκBα and phosphorylated IKK were expressed as a relative ratio of target protein to IκBα or IKK, respectively. Data are expressed as the mean ± SD (mean from three independent experiments; one-way analysis of variance followed by the least significant difference test). #$P < 0.05$, *vs.* control group; *$P < 0.05$, *vs.* OGD/R group ($n = 3$). SXT: *Shuxuetong* injection; OGD/R: oxygen-glucose deprivation/reperfusion; NF-κB: nuclear factor kappa B; IκBα: inhibitor of kappa B; IKK: I kappa B kinase.

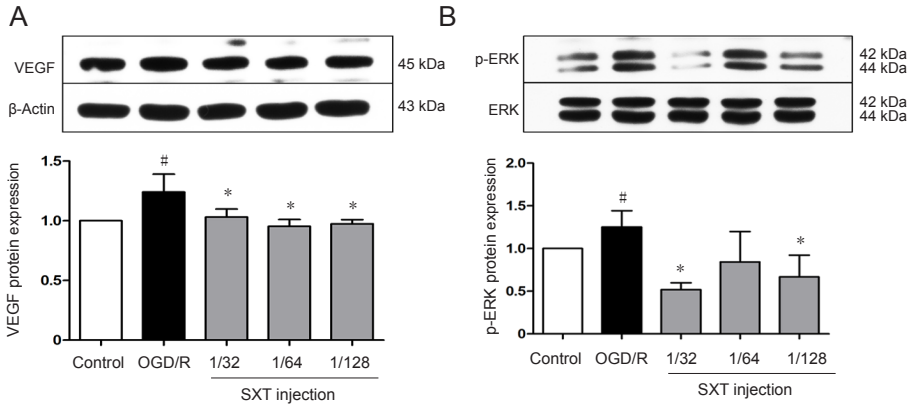

Figure 8 Effect of SXT on VEGF expression and ERK1/2 phosphorylation in bEnd.3 cells after OGD/R injury.

Cells subjected to 6-hour OGD followed by reperfusion for 18 hours were administered *Shuxuetong* injection at 1/32, 1/ 64, and 1/128 concentrations (diluted 32-, 64-, and 128-times). Protein expression levels of VEGF (A) and p-ERK1/2 (B) levels were measured by western blot assay. Relative VEGF protein expression was expressed as optical density value relative to the control group after normalizing to β-actin optical density value. Relative p-ERK1/2 protein expression was expressed as optical density value relative to control group after normalizing to ERK1/2 optical density value. Data are expressed as mean ± SD (mean from three independent experiments; one-way analysis of variance followed by least significant difference test). #$P < 0.05$, vs. control group; *$P < 0.05$ *vs.* OGD/R group ($n = 3$). SXT: *Shuxuetong* injection; OGD/R: oxygen-glucose deprivation/reperfusion; VEGF: vascular endothelial growth factor; ERK1/2: extracellular signal regulated protein kinase 1/2; p-ERK1/2: phosphorylated extracellular signal regulated protein kinase 1/2.

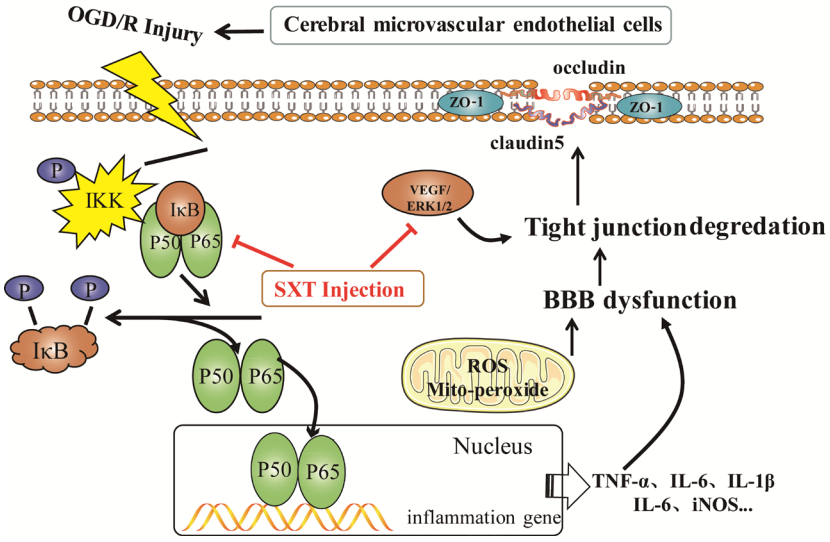

Figure 9 Possible mechanisms of SXT against OGD/R-induced BBB dysfunction in bEnd.3 cells.
SXT: *Shuxuetong* injection; OGD/R: oxygen-glucose deprivation/reperfusion; VEGF: vascular endothelial growth factor; IKK: I kappa B kinase; ERK1/2: extracellular signal regulated protein kinase 1/2; BBB: blood-brain barrier; ROS: reactive oxygen species; TNF: tumor necrosis factor; IL: interleukin; iNOS: inducible nitric oxide synthase.

al Natural Science Foundation of China, No. 81573644 (to LMH), 81573733 (to SWX); the Tianjin 131 Innovative Team Project, China (to HW); the National Major Science and Technology Project of China, No. 2012ZX09101201-004 (to SWX); the Science and Technology Plan Project of Tianjin of China, No. 16PTSYJC00120 (to LMH); the Applied Foundation and Frontier Technology Research Program of Tianjin of China (General Project), No. 14JCYBJC28900 (to SXW); the National International Science and Technology Cooperation Project of China, No. 2015DFA30430 (to HW); the Key Program of the Natural Science Foundation of Tianjin of China, No. 16ICZDJC36300 (to HW); the Scientific Research and Technology Development Plan Project of Guangxi Zhuang Autonomous Region of China, No. 14125008-2-5 (to SXW). The funders had no roles in the study design, conduction of experiment, data collection and analysis, decision to publish, or preparation of the manuscript.

Copyright license agreement: *The Copyright License Agreement has been signed by all authors before publication.*

Data sharing statement: *Datasets analyzed during the current study are available from the corresponding author on reasonable request.*

Plagiarism check: *Checked twice by iThenticate.*

Peer review: *Externally peer reviewed.*

Open access statement: *This is an open access journal, and articles are distributed under the terms of the Creative Commons Attribution-NonCommercial-ShareAlike 4.0 License, which allows others to remix, tweak, and build upon the work non-commercially, as long as appropriate credit is given and the new creations are licensed under the identical terms.*

Open peer reviewer: *Paola Bagnoli, Universita degli Studi di Pisa, Italy.*

Additional file: *Open peer review report 1.*

References

Adibhatla RM, Hatcher JF (2008) Phospholipase A(2), reactive oxygen species, and lipid peroxidation in CNS pathologies. BMB reports 41:560-567.

Amantea D, Micieli G, Tassorelli C, Cuartero MI, Ballesteros I, Certo M, Moro MA, Lizasoain I, Bagetta G (2015) Rational modulation of the innate immune system for neuroprotection in ischemic stroke. Front Neurosci 9:147.

Barreto G, White RE, Ouyang Y, Xu L, Giffard RG (2011) Astrocytes: targets for neuroprotection in stroke. Cent Nerv Syst Agents Med Chem 11:164-173.

Beker MC, Caglayan AB, Kelestemur T, Caglayan B, Yalcin E, Yulug B, Kilic U, Hermann DM, Kilic E (2015) Effects of normobaric oxygen and melatonin on reperfusion injury: role of cerebral microcirculation. Oncotarget 6:30604-30614.

Blum A, Vaispapir V, Keinan-Boker L, Soboh S, Yehuda H, Tamir S (2012) Endothelial dysfunction and procoagulant activity in acute ischemic stroke. J Vasc Interv Neurol 5:33-39.

Cao GS, Chen HL, Zhang YY, Li F, Liu CH, Xiang X, Qi J, Chai CZ, Kou JP, Yu BY (2016) YiQiFuMai Powder Injection ameliorates the oxygen-glucose deprivation-induced brain microvascular endothelial barrier dysfunction associated with the NF-kappaB and ROCK1/MLC signaling pathways. J Ethnopharmacol 183:18-28.

Chen RF, Zhang T, Sun YY, Sun YM, Chen WQ, Shi N, Shen F, Zhang Y, Liu KY, Sun XJ (2015) Oxygen-glucose deprivation regulates BACE1 expression through induction of autophagy in Neuro-2a/APP695 cells. Neural Regen Res 10:1433-1440.

Coisne C, Lyck R, Engelhardt B (2007) Therapeutic targeting of leukocyte trafficking across the blood-brain barrier. Inflamm Allergy Drug Targets 6:210-222.

da Fonseca AC, Matias D, Garcia C, Amaral R, Geraldo LH, Freitas C, Lima FR (2014) The impact of microglial activation on blood-brain barrier in brain diseases. Front Cell Neurosci 8:362.

Engelhardt B, Liebner S (2014) Novel insights into the development and maintenance of the blood-brain barrier. Cell Tissue Res 355:687-699.

Engelhardt S, Patkar S, Ogunshola OO (2014) Cell-specific blood-brain barrier regulation in health and disease: a focus on hypoxia. Br J Pharmacol 171:1210-1230.

Gerriets T, Walberer M, Ritschel N, Tschernatsch M, Mueller C, Bachmann G, Schoenburg M, Kaps M, Nedelmann M (2009) Edema formation in the hyperacute phase of ischemic stroke. Laboratory investigation. J Neurosurg 111:1036-1042.

He F, Yin F, Peng J, Li KZ, Wu LW, Deng XL (2010) Immortalized mouse brain endothelial cell line Bend.3 displays the comparative barrier characteristics as the primary brain microvascular endothelial cells. Zhongguo Dang Dai Er Ke Za Zhi 12:474-478.

Hu JL, Lin C, Li ZY (2009) Effects of Shuxuetong on blood lipid and coagulation function in patients with TIA. Zhongguo Kangfu 24:180-181.

Hung VK, Yeung PK, Lai AK, Ho MC, Lo AC, Chan KC, Wu EX, Chung SS, Cheung CW, Chung SK (2015) Selective astrocytic endothelin-1 overexpression contributes to dementia associated with ischemic stroke by exaggerating astrocyte-derived amyloid secretion. J Cereb Blood Flow Metab 35:1687-1696.

Johnston SC, Mendis S, Mathers CD (2009) Global variation in stroke burden and mortality: estimates from monitoring, surveillance, and modelling. Lancet Neurol 8:345-354.

Kago T, Takagi N, Date I, Takenaga Y, Takagi K, Takeo S (2006) Cerebral ischemia enhances tyrosine phosphorylation of occludin in brain capillaries. Biochem Biophys Res Commun 339:1197-1203.

Kaur C, Ling EA (2008) Blood brain barrier in hypoxic-ischemic conditions. Curr Neurovasc Res 5:71-81.

Kawabori M, Yenari MA (2015) Inflammatory responses in brain ischemia. Curr Med Chem 22:1258-1277.

Krueger M, Bechmann I, Immig K, Reichenbach A, Hartig W, Michalski D (2015) Blood-brain barrier breakdown involves four distinct stages of vascular damage in various models of experimental focal cerebral ischemia. J Cereb Blood Flow Metab 35:292-303.

Kuhlmann CR, Zehendner CM, Gerigk M, Closhen D, Bender B, Friedl P, Luhmann HJ (2009) MK801 blocks hypoxic blood-brain-barrier disruption and leukocyte adhesion. Neurosci Lett 449:168-172.

Li L, Xiong Y, Qu Y, Mao M, Mu W, Wang H, Mu D (2008) The requirement of extracellular signal-related protein kinase pathway in the activation of hypoxia inducible factor 1 alpha in the developing rat brain after hypoxia-ischemia. Acta Neuropathol 115:297-303.

Li V, Brustovetsky T, Brustovetsky N (2009) Role of cyclophilin D-dependent mitochondrial permeability transition in glutamate-induced calcium deregulation and excitotoxic neuronal death. Exp Neurol 218:171-182.

Liu JS, Tang D, Chen YM, Chen KL (2015) Progress in pharmacological and clinical research of Shuxuetong injection in the treatment of cardiovas-cular and cerebrovascular diseases. Zhongguo Yaoshi 18:1020-1023.

Liu YS, Qin WH (2016) Effect of Shuxuetong injection on thrombin and blood rheology of patients with cerebral infarction. Zhongguo Shequ Yishi 32:102.

Moskowitz MA, Lo EH, Iadecola C (2010) The science of stroke: mechanisms in search of treatments. Neuron 67:181-198.

Narasimhan P, Liu J, Song YS, Massengale JL, Chan PH (2009) VEGF stimulates the ERK 1/2 signaling pathway and apoptosis in cerebral endothelial cells after ischemic conditions. Stroke 40:1467-1473.

Pan B, Shi ZJ, Yan JY, Li JH, Feng SQ (2017) Long non-coding RNA NONMMUG014387 promotes Schwann cell proliferation after peripheral nerve injury. Neural Regen Res 12:2084-2091.

Pan W, Kastin AJ (2007) Tumor necrosis factor and stroke: role of the blood-brain barrier. Prog Neurobiol 83:363-374.

Preston GA, Zarella CS, Pendergraft WF, 3rd, Rudolph EH, Yang JJ, Sekura SB, Jennette JC, Falk RJ (2002) Novel effects of neutrophil-derived proteinase 3 and elastase on the vascular endothelium involve in vivo cleavage of NF-kappaB and proapoptotic changes in JNK, ERK, and p38 MAPK signaling pathways. J Am Soc Nephrol 13:2840-2849.

Roger VL, Go AS, Lloyd-Jones DM, Benjamin EJ, Berry JD, Borden WB, Bravata DM, Dai S, Ford ES, Fox CS, Fullerton HJ, Gillespie C, Hailpern SM, Heit JA, Howard VJ, Kissela BM, Kittner SJ, Lackland DT, Lichtman JH, Lisabeth LD, et al. (2012) Heart disease and stroke statistics--2012 update: a report from the American Heart Association. Circulation 125:e2-e220.

Sandoval KE, Witt KA (2008) Blood-brain barrier tight junction permeability and ischemic stroke. Neurobiol Dis 32:200-219.

Shin JA, Oh S, Ahn JH, Park EM (2015a) Estrogen receptor-mediated resveratrol actions on blood-brain barrier of ovariectomized mice. Neurobiol Aging 36:993-1006.

Shin JA, Yoon JC, Kim M, Park EM (2016) Activation of classical estrogen receptor subtypes reduces tight junction disruption of brain endothelial cells under ischemia/reperfusion injury. Free Radic Biol Med 92:78-89.

Shin JA, Kim YA, Jeong SI, Lee KE, Kim HS, Park EM (2015b) Extracellular signal-regulated kinase1/2-dependent changes in tight junctions after ischemic preconditioning contributes to tolerance induction after ischemic stroke. Brain Struct Funct 220:13-26.

Suchadolskiene O, Pranskunas A, Baliutyte G, Veikutis V, Dambrauskas Z, Vaitkaitis D, Borutaite V (2014) Microcirculatory, mitochondrial, and histological changes following cerebral ischemia in swine. BMC Neurosci 15:2.

Tuttolomondo A, Pecoraro R, Pinto A (2014) Studies of selective TNF inhibitors in the treatment of brain injury from stroke and trauma: a review of the evidence to date. Drug Des Devel Ther 8:2221-2238.

Wang CP, Li GC, Shi YW, Zhang XC, Li JL, Wang ZW, Ding F, Liang XM (2014a) Neuroprotective effect of schizandrin A on oxygen and glucose deprivation/reperfusion-induced cell injury in primary culture of rat cortical neurons. J Physiol Biochem 70:735-747.

Wang L, Chen M, Yuan L, Xiang Y, Zheng R, Zhu S (2014b) 14,15-EET promotes mitochondrial biogenesis and protects cortical neurons against oxygen/glucose deprivation-induced apoptosis. Biochem Biophys Res Commun 450:604-609.

Wang LF, Li X, Gao YB, Wang SM, Zhao L, Dong J, Yao BW, Xu XP, Chang GM, Zhou HM, Hu XJ, Peng RY (2015) Activation of VEGF/Flk-1-ERK pathway induced blood-brain barrier injury after microwave exposure. Mol Neurobiol 52:478-491.

Watanabe T, Dohgu S, Takata F, Nishioku T, Nakashima A, Futagami K, Yamauchi A, Kataoka Y (2013) Paracellular barrier and tight junction protein expression in the immortalized brain endothelial cell lines bEND.3, bEND.5 and mouse brain endothelial cell 4. Biol Pharm Bull 36:492-495.

Wei H, Leeds P, Chen RW, Wei W, Leng Y, Bredesen DE, Chuang DM (2000) Neuronal apoptosis induced by pharmacological concentrations of 3-hydroxykynurenine: characterization and protection by dantrolene and Bcl-2 overexpression. J Neurochem 75:81-90.

Won S, Sayeed I, Peterson BL, Wali B, Kahn JS, Stein DG (2015) Vitamin D prevents hypoxia/reoxygenation-induced blood-brain barrier disruption via vitamin D receptor-mediated NF-kB signaling pathways. PLoS One 10:e0122821.

Wu C, Li D, Jia W, Hu Z, Zhou Y, Yu D, Tong T, Wang M, Lin D, Qiao Y, Zhou Y, Chang J, Zhai K, Wang M, Wei L, Tan W, Shen H, Zeng Y, Lin D (2013) Genome-wide association study identifies common variants in SLC39A6 associated with length of survival in esophageal squamous-cell carcinoma. Nat Genet 45:632-638.

Xing C, Arai K, Lo EH, Hommel M (2012) Pathophysiologic cascades in ischemic stroke. Int J Stroke 7:378-385.

Xu R, Feng X, Xie X, Zhang J, Wu D, Xu L (2012) HIV-1 Tat protein increases the permeability of brain endothelial cells by both inhibiting occludin expression and cleaving occludin via matrix metalloproteinase-9. Brain Res 1436:13-19.

Yang Y, Rosenberg GA (2011) Blood-brain barrier breakdown in acute and chronic cerebrovascular disease. Stroke 42:3323-3328.

Yin XH (2011a) Effect of Shu Xue Tong Injection on neural function and hemorheology in patients with acute ischemic stroke. Zhongguo Yiyao Daobao 8:52-53.

Yin YS (2011b) Shuxuetong injection pharmacological effects and clinical application of new advances. Linchuang Yixue Gongcheng 18:472-473.

Young PP, Fantz CR, Sands MS (2004) VEGF disrupts the neonatal blood-brain barrier and increases life span after non-ablative BMT in a murine model of congenital neurodegeneration caused by a lysosomal enzyme deficiency. Exp Neurol 188:104-114.

Zehendner CM, Librizzi L, de Curtis M, Kuhlmann CR, Luhmann HJ (2011) Caspase-3 contributes to ZO-1 and Cl-5 tight-junction disruption in rapid anoxic neurovascular unit damage. PLoS One 6:e16760.

Zhang YK, Yang JH, Gao F, Duan FY (2017) Effect of Buyang Huanwu decoction combined with bone marrow mesenchymal stem cell transplantation on expression of integrin in a rat model of middle cerebral artery occlusion. Zhongguo Zuzhi Gongcheng Yanjiu 38:724-729.

Zhang ZG, Zhang L, Jiang Q, Zhang R, Davies K, Powers C, Bruggen N, Chopp M (2000) VEGF enhances angiogenesis and promotes blood-brain barrier leakage in the ischemic brain. J Clin Invest 106:829-838.

P-Reviewer: Bagnoli P; C-Editor: Zhao M; S-Editors: Yu J, Li CH; L-Editors: James R, Hindle A, Qiu Y, Song LP; T-Editor: Liu XL